PAGE21 WP5

Land surface hydrology from remotely sensed data at PAGE21 sites

VIENNA UNIVERSITY OF TECHNOLOGY
DEPARTMENT OF GEODESY AND GEOINFORMATION
RESEARCH GROUPS PHOTOGRAMMETRY & REMOTE SENSING

ALFRED-WEGENER-INSTITUT
HELMHOLTZ-ZENTRUM FÜR POLAR- UND MEERESFORSCHUNG

2014 July

This document is the documentation for the version 1 release of the land surface hydrology maps from remotely sensed data at PAGE21 sites. It has been compiled for the PAGE21 project (FP7-ENV-2011 GRANT AGREEMENT NO: 282700), a project coordinated by the Alfred-Wegener-Institute for Polar and Marine Research. It is based on the Milestone document #36 'Datasets and documentation: high to medium resolution remotely sensed results'

Consortium member:

Department of Geodesy and Geoinformation (GEO)
Research Group Remote Sensing
Vienna University of Technology
Gusshausstrasse 27-29/E122
1040 Vienna, Austria

permafrost@ipf.tuwien.ac.at
www.geo.tuwien.ac.at

Status:	Issue 1.0
Authors:	Widhalm, B. (TUW), Högström, E.(TUW), Ressl, C.(TUW), Trofaier, A. M.(TUW), Heim, B. (AWI), Biasi, C. (UEF), Bartsch, A.(TUW),
Circulation:	PAGE21, Pangaea
Amendments:	

Issue	*Date*	*Details*	*Editor*
Issue 1.0	2014-07-17	V1 Data documentation extracted from Milestone document 36 and 37	AB

1 Contents

2 Dataset overview

Land surface hydrology is characterized at selected sites (area extent up to 400 km²) in arctic and sub-arctic environments by (1) open water classification at a range of spatial resolutions (nominal 3m from ALOS PRISM, 10 m from ALOS AVNIR, ~7/16m from ALOS PALSAR fine beam), (2) the topographic wetness index (based on 10m DEMs from ALOS PRISM where available, or the 90 m ESA DUE Permafrost dataset) and (3) seasonal inundation dynamics (75m from ENVISAT ASAR Wide swath).

The datasets are available as GeoTIFFs grouped by site and include documentation, validation results and an overview map as png at selected sites. The dataset has been compiled as part of the PAGE21 WP5 'Multi-scale integration and remote sensing'.

ALOS datasets have been available through JAXA PI agreements #80, and #1200 by Vienna University of Technology.

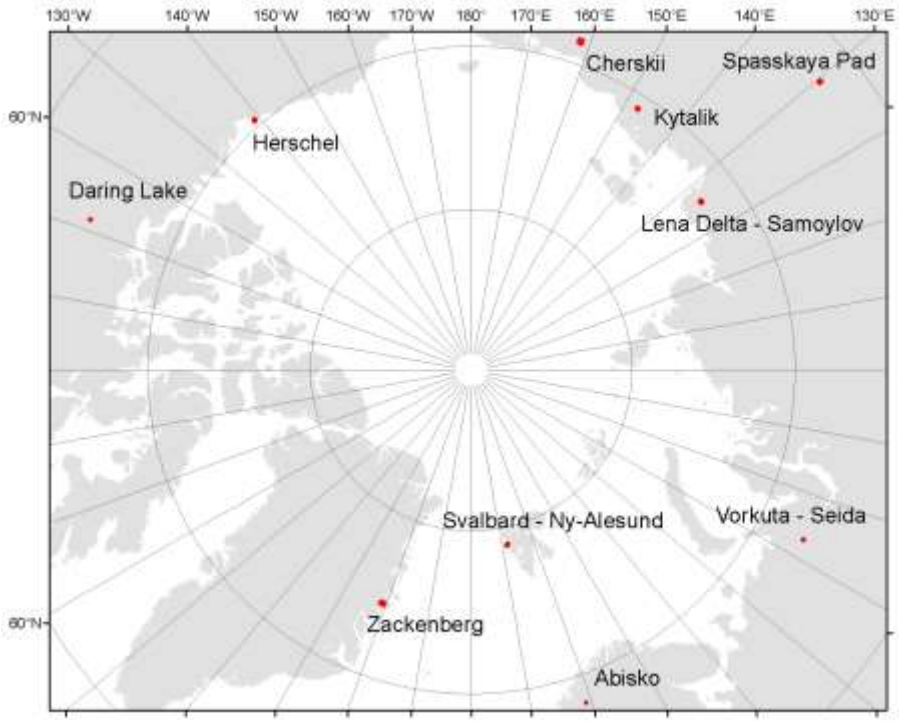

Figure 1
Overview of PAGE21 sites (primary and secondary) with data availability

3 Data specification

3.1 File naming

OOO_SSSSS_PPP_VVV_YYYYMMDD_ROI.EEE

Where OOO="organisation", e.g. TUW,AWI
SSSSSS="sensor and mode"
PPP="product"
VVV="product version"
YYYYMMDD= "acquisition date and time"
(or year range YYYY_YYYY)
ROI="region/site of interest"
EEE="file extension", e.g. tif

Sensor/source codes

ALOS PALSAR FBD - PALFD
ALOS PRISM - APRISM
ALOS AVNIR - AAVNIR
ENVISAT ASAR WS - ASARWS
Rapid Eye - RAPEYE
ESA DUE Permafrost DEM - DUEDEM

Product codes

WBO Water bodies
DEM Elevation
CHA Champfer file for DEM
(see Ressl & Bartsch (2012) for explanation)
CTI Compound topographic wetness index

Site codes

ABI Abisko
CHE Cherskii
DAR Daring lake
HER Herschel Island
KYT Kytalik
LEN Lena delta
NYA Ny Alesund
SPA Spasskaya Pad
VOR Vorkuta Saida
ZAC Zackenberg

3.2 Site boundaries and projections

Table 1: Site extents (decimal degree) and used projections (all WGS84)

	Latitude min	Longtitude min	Latitude max	Longtitude max	Projections used
ABI	68.28	18.93	68.37	19.18	UTM Zone 34N, UPS North
CHE	68.52	161.25	68.77	161.95	UTM Zone 72N, UPS North
DAR	64.80	-111.68	64.89	-111.46	UTM Zone 12N, UPS North
HER	69.5	-139.29	69.67	-138.82	UTM Zone 7N, UPS North
KYT	70.77	147.26	70.91	147.78	UTM Zone 55N, UPS North
LEN	72.28	126.01	72.46	126.62	UTM Zone 52N, UPS North
NYA	78.86	11.32	78.98	12.09	UTM Zone 33N, UPS North
SPA	62.21	129.41	62.40	129.77	UTM Zone 52N, UPS North
VOR	67.01	62.85	67.10	63.08	UTM Zone 41N, UPS North
ZAC	74.44	-21.46	74.64	-20.28	UTM Zone 27N, UPS North

3.3 Open water bodies

Monitoring of water bodies is relevant to geomorphology (thaw lakes related to thermokarst), soils and fluxes (temporary and permanent water logged conditions). Remotely sensed data have been used to characterize the distribution with respect to spatial scales (Muster et al. 2012, 2013) as well as the seasonal and intra-annual dynamics (Bartsch et al. 2012, Trofaier et al. 2013, Reschke et al. 2012). The identification of the latter is crucial when lakes area used to quantify long-term changes related to permafrost degradation. The site specific water fractions and number of lakes has been therefore determined for all PAGE21 sites where sufficient have been available using multi-resolution satellite data (nominal resolutions of 2.5/3m, 10m, ~7 /16m, 75m).

Seasonal and inter-annual variations in inundation are characteristic for the sites located in the Siberian lowland areas. Temporal water logging has been specifically identified for Kytalik, Cherskii, Lena Delta and Spasskaja Pad. Maps of seasonal changes and/or (depending on data availability) inter-annual variations in summer conditions are based on ENVISAT ASAR WS time series analyses over entire Northern Siberia (methods and valida-

tion in Bartsch et al. 2012, Trofaier et al. 2013, Reschke et al. 2012, ESA STSE ALANIS Project).

ALOS PALSAR, AVNIR and PRISM scenes were classified for open water extent at specific dates. ENVISAT ASAR WS products represent aggregations over either specific months (date code e.g. for July 2007 20070700) or summer maximum open water extended summed over several years (date code for 2007 – 2011: 2007_2011; source ESA DUE Permafrost project).

The areas of each water body polygon was calculated and a summary of the area statistics from the ALOS sensors as well as ALANIS product and are shown in Table 2 - Table 5. For accuracy assessment, 30 points were selected randomly for each site and compared with reference data (google earth). The number of correctly classified points out of 30 is presented in the last column.

Table 2: General water body area statistics from the ALOS PALSAR WBO product. The unit is square kilometres (km^2) in column 2 - 5. Count indicates the total number of water bodies. The last column indicates the number of correctly classified points out of 30 randomly chosen ones within the area.

	average	median	max	min	count	accuracy (%)
VOR	0,0031	0,0016	0,1292	0,0004	353	100
CHE	0,0779	0,0035	46,6925	0,0003	1439	100
SPA	0,0177	0,0023	1,2045	0,0003	562	100
DAR	0,2531	0,0052	15,6168	0,0004	124	90
NOS	0,0172	0,0015	2,4717	0,0003	712	97
KYT	0,0623	0,0018	6,6430	0,0003	1175	100
HER	0,0018	0,0010	0,0856	0,0003	747	90
LEN	0,0018	0,0003	1,9563	0,0001	24320	90
ZAC	0,0636	0,0101	4,7661	0,0025	414	93
ABI	0,2104	0,0042	13,3936	0,0002	70	97
NYA	0,0341	0,0148	0,2448	0,0106	91	89

Table 3: General water body area statistics from the ALOS AVNIR WBO product. The unit is square kilometres (km^2) in column 2 - 5. Count indicates the total number of water bodies. The last column indicates the percentage of correctly classified points out of 30 randomly chosen ones within the area

	average	median	max	min	count	accuracy (%)
VOR	0,002	0,000	0,113	0,000	315	100
SPA	0,002	0,000	0,594	0,000	750	97
KYT	0,062	0,000	10,165	0,000	1101	97
LEN	0,004	0,000	1,960	0,000	4808	96
ABI	0,1391	0,0026	14,5185	0,0001	119	97

Table 4: General water body area statistics from the ALOS PRISM WBO product. The unit is square kilometres (km^2) in column 2 - 5. Count indicates the total number of water bodies. The last column indicates percentage of correctly classified points out of 30 randomly chosen ones within the area.

	average	median	max	min	count	accuracy (%)
VOR	0,00053469	0,000036	0,120375	0,000009	2149	100
CHE	0,00205175	0,000009	3,29081	0,000009	34258	97
KYT	0,001339	0,000018	5,679320	0,000003	38169	97
LEN	0,000095	0,000009	4,79759	0,000009	380207	90

Table 5: General water body area statistics from the ALANIS WBO product (monthly aggregated product for July 2007). The unit is square kilometres (km^2) in column 2 - 5. Count indicates the total number of water bodies. The column TWL shows the temporary waterlogged area, calculated as the total water body extent difference June - August. The last column indicates percentage of correctly classified points out of 30 randomly chosen ones within the area.

	average	median	max	min	count	TWL (%)	accuracy
CHE	0,1639	0,0555	3,2358	0,0056	292	5,3 (2007)	93
KYT	0,1219	0,0167	4,6123	0,0056	226	17,5 (2008)	83
LEN	0,0668	0,0111	1,5929	0,0056	304	-	88

3.4 Topographic wetness index

A circumpolar DEM at 100 m resolution is available from the ESA DUE Permafrost project (Santoro and Wiesmann 2012). Subsets of the DUE Permafrost elevation model have been used for satellite data pre-processing (orthorectification) as well as for the retrieval of the Topographic Wetness Index where no ALOS PRISM data have been available. Resolution is 3'', similar to that of SRTM. This DEM is based on the following sources:

- SRTM-3 DEM (Shuttle Radar Topography Mission) up to 60º latitude;
- RTM (Russian Topographic Maps, contour lines) for much of Western Europe and Asia;
- CDED (Canada Digital Elevation Data);
- U.S. Geological Survey DEM (for Alaska);

It has been used for site scale derivation of terrain parameters and will be used for up-scaling purposes. Further on ALOS PRISM data have been obtained for several sites. They can be used for stereophotogrammetric processing which is described below.

Local scale photogrammetric processing of ALOS-Prism Triplets (ground sampling distance 2.5m, Ressl & Bartsch 2012) has been carried out for five PAGE21 sites. ERDAS LPS has been used for surface point extraction and OPALS for surface interpolation. The 'orientation was carried out with LPS supported by ground control points (GCPs) and tie points. The GCPs were obtained in Google Earth (longitude, latitude) – thus with limited quality. The GCP's heights were therefore extracted from the DUE Permafrost DEM (Santoro & Wiesman 2012) and processed with LPS. Eventually DEMs with raster size 10m were interpolated from these points using the software OPALS (developed at TU Wien). The gap areas in between were filled using a TIN-approach. In a post processing step the DEMs have been adjusted to the Reference DEM (DUE Permafrost DEM; 2m Canada DEM for Herschel Island available through AWI)

From the images surface points can only be extracted where the image contrast is large enough, therefore the distribution of the extracted surface points depends on the image content and will vary over the area. Thus the quality of the surface description (its resolution) is not homogenous over the area. The grid width used for the DEM is 10m (which is 4 times the ground sampling distance of the original ALOS images of 2.5m). In order to document the quality of the surface description a so-called chamfer image was created also which is co-registered to the DEM. The chamfer image stores in each cell the distance to the closest cell which contains extracted surface points. Data acquired before 2007 (Kytalik only) are impacted by radiometric variations (stripes) which could only partly corrected (Figure 2). This especially impacts the retrieval of derivatives. The mean elevation difference compared to GPS measurements is below 1m nevertheless (**Table 6:** Elevation difference in m between the DUE Permafrost (+ Lidar DEM for Herschel) and PRISM DEMs (DUE-PRISM (water-masked))

	Mean	Standard deviation
CHE	1.04	5.95
HER (DUE)	-26,50	28,32
HER (LIDAR)	0.92	3,99
KYT	-1,00	4,63
VOR	3,46	5,43
ZAC	-4,23	30,90

Table 7). The results have been validated using the DUE Permafrost DEM (Table 6) as well as in-situ GPS measurements available within the project consortium, specifically UEF and TU Wien (Table 6: Elevation difference in m between the DUE Permafrost (+ Lidar DEM for Herschel) and PRISM DEMs (DUE-PRISM (water-masked))

	Mean	Standard deviation
CHE	1,04	5,95
HER (DUE)	-26,50	28,32
HER (LIDAR)	0.92	3,99
KYT	-1,00	4,63
VOR	3,46	5,43
ZAC	-4,23	30,90

Table 7). The elevation characteristics for each site are summarized in

Table 7.

Table 6: Elevation difference in m between the DUE Permafrost (+ Lidar DEM for Herschel) and PRISM DEMs (DUE-PRISM (water-masked))

	Mean	Standard deviation
CHE	1,04	5,95
HER (DUE)	-26,50	28,32
HER (LIDAR)	0.92	3,99
KYT	-1,00	4,63
VOR	3,46	5,43
ZAC	-4,23	30,90

Table 7: Accuracy assessment of PRISM DEMs with GPS measurements (in m; GPS-PRISM DEM)

	GPS points #	mean	std	min	max	median
Vorkuta	12	5,89	1,99	3,04	8,63	5,91
Kytalyk	210	-0,86	5,31	-14,61	24,66	-0,63

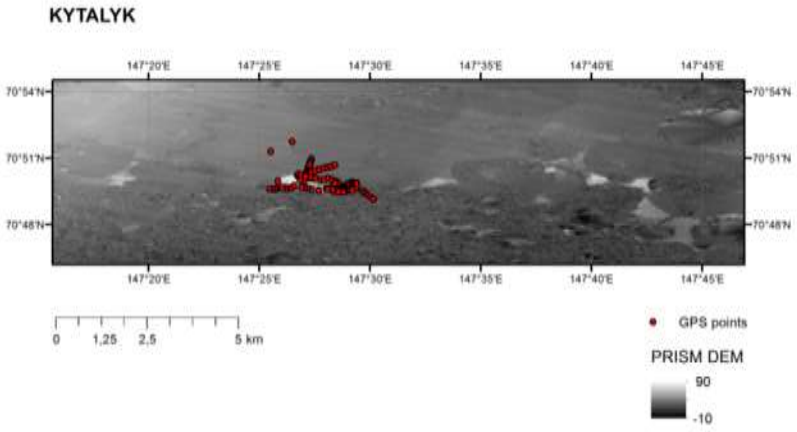

Figure 2: Location GPS measurements – Kytalik

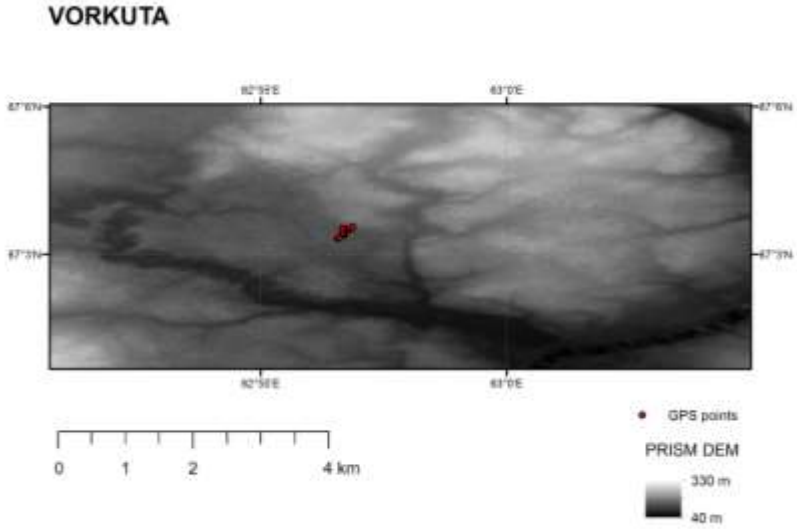

Figure 3: Location GPS measurements – Vorkuta

Table 8: Terrain data summary

Site	DUE Permafrost DEM			PRISM DEM		
	Range	Mean	STD	Range	Mean	STD
LEN	1 - 56	14,1	12,5			
ABI	340 – 1255	661,5	235,0			
KYT	2 - 40	8,5	3,8	(-13,6) - 37,1	9,3	5,4
CHE	1 - 633	57,2	73,0	(-21,8) – 622,6	54,5	72,3
VOR	63 - 161	106,9	21,9	47,8 – 160,6	103,1	21,6
SPA	91 - 231	200,1	33,1			
NYA	1 - 768	201,3	173,1			
ADV	1 - 255	204,9	86,1			
ZAC	1 - 1424	527,3	318,8	(-10,7) –	520,2	324,2
DAR	384 - 482	439,0	18,5			
HER	2 - 166	60,3	49,3	(-9,9) – 183,4	69,0	36,6
NOS	2 - 25	11,6	4,2			

Wetness plays an important role for up-scaling of soil parameters and fluxes. In addition to surface moisture retrievals from microwave satellite data, the compound topographic wet-

ness index (CTI) has been derived from ALOS PRISM as well as the DUE DEM. For the calculation of the compound topographic (wetness) index, the following DEM data derivatives are needed:

- Flow Directions: The flow direction data layer defines the direction of flow from each cell in the DEM to its steepest down-slope neighbour. Values of flow direction vary from 1 to 255. Defined flow directions follow the convention adopted by ARC/INFO's flow direction implementation.
- Flow Accumulations (FA): The flow accumulation data layer defines the amount of upstream area draining into each cell. It is essentially a measure of the upstream catchment area. The flow direction layer is used to define which cells flow into the target cell. To receive the drainage areas in square meters the flaw accumulation has to be scaled by the cell size.
- Slope: The slope data layer describes the maximum change in the elevations between each cell and its eight neighbours. The slope is expressed in integer degrees of slope between 0 and 90.

The Compound Topographic Index (CTI), commonly referred to as the Wetness Index, is a function of the upstream contributing area and the slope of the landscape. The implementation is based on Moore et al (1991). The CTI is calculated using the flow accumulation (FA) layer along with the slope as:

$$CTI = \ln (FA / \tan (slope))$$

In areas of no slope, a CTI value is obtained by substituting a slope of 0.001. Examples are shown in Figure 4. The DEMs were processed in metric coordinate systems in order to receive reasonable drainage area results. Sinks were filled in the DEMs and the slope values were converted into radians for deriving the tangent.

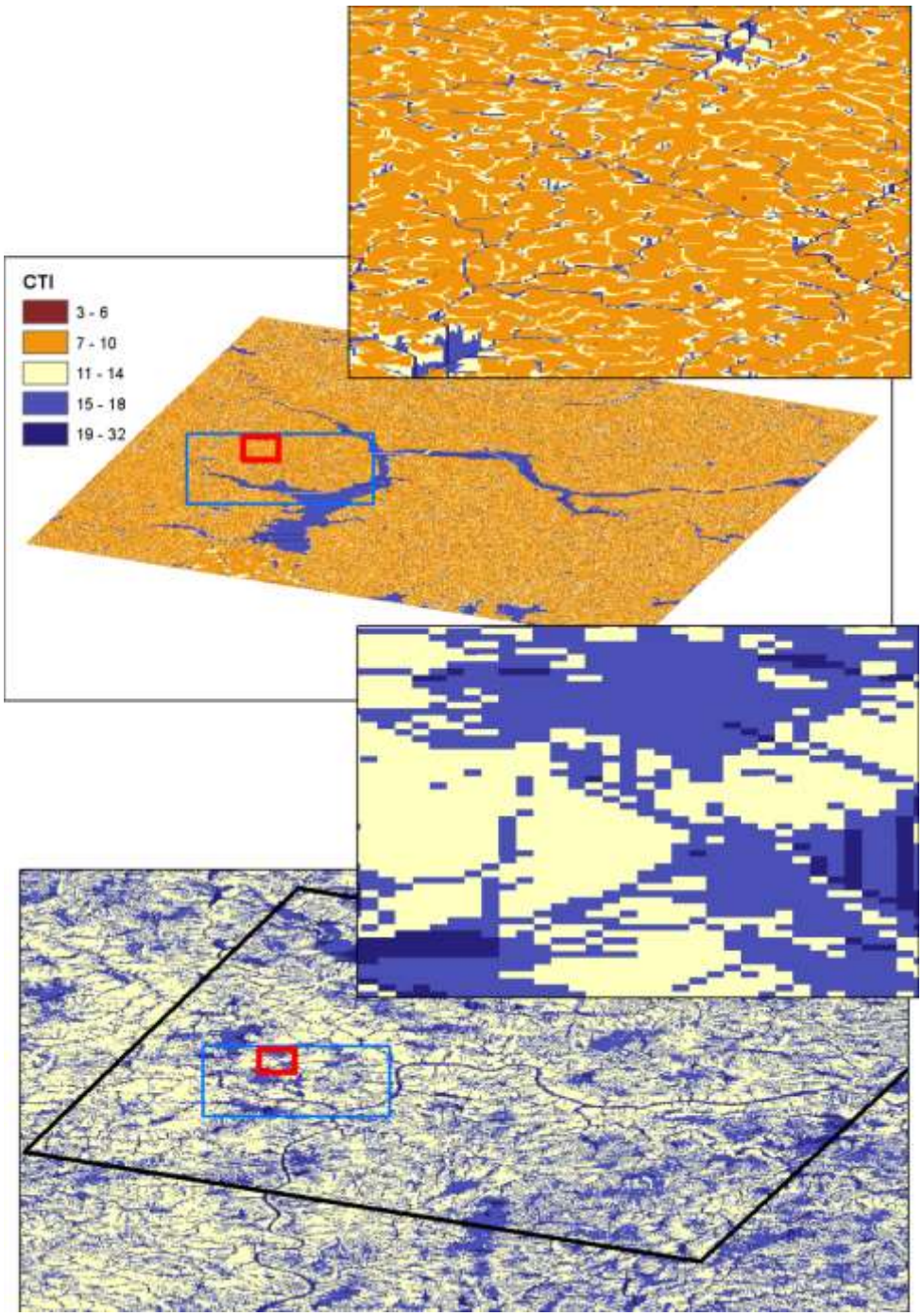

Figure 4: Example of the Compound Topographic wetness index (CTI) for Vorkuta: top PRISM, bottom DUE DEM (same units; blue boundary – site extent)

4 Data access and contact information

Data can be accessed via PANGAEA (http://doi.pangaea.de/10.1594/PANGAEA.834200) and should be cited as:
Widhalm, B; Högström, Elin; Ressl, Camillo; Trofaier, Anna Maria; Heim, Birgit; Biasi, C; Bartsch, Annett (2014): Land surface hydrology from remotely sensed data at PAGE21 sites. DOI:10.1594/PANGAEA.834200

For questions about the dataset, contact Annett.Bartsch@tuwien.ac.at.

Additional information on the Project can be found at www.page21.eu

5 References

Bartsch A., Kidd R., Pathe C., Wagner W., and K. Scipal (2007): Satellite radar imagery for monitoring inland wetlands in boreal and sub-arctic environments. Journal of Aquatic Conservation: Marine and Freshwater Ecosystems 17: 305-317, DOI: 10.1002/aqc.836.

Bartsch A., Pathe C., Wagner W., and K. Scipal (2008): Detection of permanent open water surfaces in central Siberia with ENVISAT ASAR wide swath data with special emphasis on the estimation of methane fluxes from tundra wetlands. Hydrology Research 39 (2): 89-100. doi:10.2166/nh.2008.041

Bartsch, A., Trofaier, A., Hayman, G., Sabel, D., Schlaffer, S., Clark D. & E. Blyth (2012): Detection of open water dynamics with ENVISAT ASAR in support of land surface modelling at high latitudes; Biogeosciences, 9, 703-714. doi:10.5194/bg-9-703-2012.

Moore, I. D., Grayson, R. B., and Ladson, A. R.: Digital terrain modeling – a review of hydrological, geomorphological, and biological applications, Hydrol. Processes, 5, 3–30, 1991.

Muster, S., Heim, B., Abnizova, A. and J. Boike (2013): Water Body Distributions Across Scales: A Remote Sensing Based Comparison of Three Arctic Tundra Wetlands Remote Sens. 2013, 5(4), 1498-1523.

Reschke J., Bartsch A., Schlaffer S., Schepaschenko D (2012). Capability of C-Band SAR for Operational Wetland Monitoring at High Latitudes. Remote Sensing 4(10):2923-2943. doi:10.3390/rs4102923

Ressl, Camillo; Bartsch, Annett (2012): ALOS Digital Elevation Models with links to geotiff files. Department of Geodesy and Geoinformatics, TU Vienna, doi:10.1594/PANGAEA.783306

Santoro, Maurizio; Strozzi, Tazio (2012): Circumpolar digital elevation models > 55 N with links to geotiff images, GAMMA Remote Sensing, doi:10.1594/PANGAEA.779748. In: DUE Permafrost Project Consortium (2012): ESA Data User Element (DUE) Permafrost: Circumpolar Remote Sensing Service for Permafrost (Full Product Set) with links to datasets. doi:10.1594/PANGAEA.780111

Schlaffer, Stefan; Sabel, Daniel; Bartsch, Annett; Wagner, Wolfgang (2012): Regional water bodies remote sensing products with links to geotiff images. doi:10.1594/PANGAEA.779754

Trofaier, A.M., Rees, G., Bartsch, A., Sabel, D., Schlaffer, S. (2012): Feasibility Study of Using Active Microwave Data for Examination of Thaw Lake Drainage Patterns over the Yamal Peninsula. Proceedings of the Tenth International Conference on Permafrost, volume 1, Salekhard 2012, 413-418.

Trofaier A. M., Bartsch, A., Rees, G. & M. Leibman (2013): Assessment of spring floods and surface water extent over the Yamalo-Nenets Autonomous District. Environ. Res. Lett. 8 045026 doi:10.1088/1748-9326/8/4/045026

Anna Maria Trofaier, William Gareth Rees, and Annett Bartsch (2013): ARCTIC WATER BODY DYNAMICS: A PAN-SIBERIAN STUDY OF SEASONAL CHANGES IN INUNDATION - STAGE 1: YAMALO-NENETS AUTONOMOUS DISTRICT. In: Proceedings of the ESA Living Planet Symposium. 2013', Edinburgh, UK, 9–13 September 2013 (ESA SP-722, December 2013), 4 pages